Electronic Supplementary Information

Title: Gaining control on optical force by the stimulated-emission resonance effect.

Authors: Tetsuhiro Kudo,[1*] Boris Louis,[2,3] Hikaru Sotome,[4] Jim Jui-Kai Chen,[2] Syoji Ito,[4,5*] Hiroshi Miyasaka,[4] Hiroshi Masuhara,[6,7*] Johan Hofkens,[2,8*] Roger Bresolí-Obach[2,9*]

Affiliation:

[1] Laser Science Laboratory, Toyota Technological Institute, Hisakata, Tempaku-ku, Nagoya 468-8511, Japan.

[2] Laboratory for Photochemistry and Spectroscopy, Division for Molecular Imaging and Photonics, Department of Chemistry, Katholieke Universiteit Leuven, Belgium.

[3] Division of Chemical Physics and NanoLund, Lund University, P.O. Box 124, Lund, Sweden.

[4] Division of Frontier Materials Science and Center for Promotion of Advanced Interdisciplinary Research, Osaka University, Toyonaka, Osaka 560-8531, Japan.

[5] Research Institute for Light-induced Acceleration System (RILACS), Osaka Metropolitan University, 1-2, Gakuen-cho, Naka-ku, Sakai, Osaka 599-8570, Japan.

[6] Department of Applied Chemistry, College of Science, National Yang Ming Chiao Tung University, Hsinchu, Taiwan.

[7] Center for Emergent Functional Matter Science, National Yang Ming Chiao Tung University, Hsinchu, Taiwan.

[8] Max Planck Institute for Polymer Research, Mainz 55128, Germany.

[9] AppLightChem, Institut Químic de Sarrià, Universitat Ramon Llull, Barcelona, Catalunya, Spain.

E-mail corresponding authors:

T.K. kudo@toyota-ti.ac.jp; S.I. sito@chem.es.osaka-u.ac.jp; H.M. masuhara@masuhara.jp; J.H. johan.hofkens@kuleuven.be; R.B-O. roger.bresoli@iqs.edu

Materials and methods

Synthesis of the dye-doped BP-PDI polystyrene particles

The synthetic methodology was adapted from reference.[1] Specifically, 50 μL of commercial 1000 nm bare polystyrene particles (PS MPs; 2.5% w/w; Polybead® Carboxylate Microspheres; Ref: 08226-15; Polysciences) were diluted with 200 μL of miliQ water. Independently, 0.25 mg of perylenediimide derivative (BP-PDI; Figure 1) was dissolved in 1 mL of tetrahydrofuran (THF) to yield a roughly 0.25 mM BP-PDI concentration. 65 μL of the BP-PDI solution was added to the diluted PS MPs solution. After 10 minutes, 350 μL of miliQ water was added in the mixture and the MPs were recovered by centrifugation at 5000g for 5 minutes. Afterwards, the MPs were re-suspended with 250 mL of miliQ water and sonicated for 5 minutes. The dyeing procedure was repeated for 5 complete cycles. Finally, the MPs were washed three times with 500 μL of miliQ water and stored at 4 $^{\circ}$C.

Transient absorption spectroscopy

Transient absorption spectra of BP-PDI were measured using a home-built setup. The pulsed light source was a Ti:sapphire regenerative amplifier (Spectra-Physics, Spitfire, 802 nm, 100 fs, 1 mJ, 1 kHz) seeded by a Ti:sapphire oscillator (Spectra-Physics, Tsunami, 802 nm, 100 fs, 650 mW, 80 MHz). The output was equally split into two portions, each of which was introduced into two optical parametric amplifiers (Light-Conversion, TOPAS-Prime). The first OPA generated the excitation pulse at 580 nm, and the second one generated the probe pulse at 1180 nm. This near-infrared pulse was focused into a 2 mm CaF_2 plate and converted to white light continuum ranging in 350-1100 nm, which was further divided into the signal and reference pulses. The signal one was guided into the sample cell and the reference one was used for the compensation of the intensity fluctuation of the probe pulse. Both the pulses were detected with multichannel photodiode arrays (Hamamatsu, PMA-10). The delay time between the excitation and probe pulses was controlled with an optical delay stage. The polarization of the excitation pulse was set to the magic angle with respect to that of the probe pulse. The time resolution of the measurements was typically 150 fs. The sample solution was set in a rotation cell with an optical length of 2 mm.

The quantitative determination of the molar absorption coefficient of BP-PDI in the S_1 state is essential for the calculation of optical force, although the excitation condition such as spot size of the excitation pulse is often difficult to precisely evaluate in transient absorption spectroscopy. To this end, we used a standard sample (ZnTPP in DMF) whose absorption coefficient in the excited state was already determined,[2] and measured its transient absorption spectra under the completely same experimental condition as BP-PDI. Under this condition, the relation of transient absorbance of BP-PDI and standard sample is described in Equation S1:

$$\frac{\Delta A_{\text{BPPDI}}}{\Delta A_{\text{Std}}} = \frac{(\varepsilon_{\text{BPPDI\_ex}} - \varepsilon_{\text{BPPDI\_gr}})}{(\varepsilon_{\text{Std\_ex}} - \varepsilon_{\text{Std\_gr}})} \cdot \frac{(1 - 10^{-A_{\text{BPPDI}}})}{(1 - 10^{-A_{\text{Std}}})} \qquad \textbf{\textit{Eq. S1}}$$

Here, ΔA_{BPPDI} and ΔA_{Std} are transient absorbance detected in the measurements. A_{BPPDI} and A_{Std} are absorbance of the sample solutions at the excitation wavelength obtained from steady-state absorption spectra. $\varepsilon_{\text{BPPDI\_gr}}$ and $\varepsilon_{\text{BPPDI\_ex}}$ are molar absorption coefficients of BPPDI in the ground and excited states. $\varepsilon_{\text{Std\_gr}}$ and $\varepsilon_{\text{Std\_ex}}$ are molar absorption coefficients of the standard sample in the ground and excited states. The parameters except for $\varepsilon_{\text{BPPDI\_ex}}$ are experimentally obtained or available in the reference. On the basis of the above equation and parameters, $\varepsilon_{\text{BPPDI\_ex}}$ was quantitatively determined. In addition, the excitation power dependence was investigated so as to exclude an effect of absorption saturation, and the linearity of transient absorbance against the excitation power was confirmed in the measurements.

Sample preparation for optical trapping
Before preparing the sample, the aqueous BP-PDI labeled MPs suspension was sonicated for 15 minutes and diluted to a concentration of 7×10^6 MPs/mL. The glass coverslips were cleaned using a heat treatment (>24 hours, 450 °C), followed by an ozone treatment (60 min). For the sample preparation, 8 µL of the MPs suspension were added to a small chamber (Grace Bio-Labs) and glued onto a clean coverslip. The chamber was immediately sealed with an additional clean coverslip to prevent solvent evaporation.

Optical setup
All experiments were conducted on a home-built widefield inverted microscope (Figure S4) as previously reported.[3] A 1064 or 640 nm continuous-wave trapping laser was focused at the upper glass/solution interface using a water-immersion 60x objective (Olympus; UPlanSApo60XW NA 1.20). Meanwhile, the other lasers (561 and 640 nm) were focused at the back aperture of the objective to achieve widefield illumination at the glass/solution interface with an excitation power density up to 20×10^3 W/cm^2. The emitted or transmitted light is collimated by the objective; guided towards the detection path where the signal is filtered from excitation laser light using an appropriate bandpass filter; and projected onto a sCMOS camera by a tube lens. The particle movement was recorded as transmission or fluorescence images and the particle trajectories are tracked as previously described.[4] We estimated the trapping stiffness by fitting Hooke's restoring force law to the particle motion (see next section).[5]

Calculation of the trapping stiffness
When a particle is subjected to the intense laser field from the optical trap, it will experience multiple forces, including the scattering, the gradient, and the resonant forces. The particle will

then be in a potential well which will depend on the laser field intensity and intensity distribution. Comparable to a spring, when the particle moves too far from the equilibrium position, it is rapidly restored back to the equilibrium position. Therefore, by analyzing the particle motion inside the potential well we can have an idea of how strong in the optical trap which we refer to as the optical trapping stiffness in parallel with the spring analogy (Figure S6).

For motion close to the center of the trap, we can approximate the behavior as linear spring at the trapping center. Following the equipartition theorem, the energy of the Brownian motion should be equal to the energy stored in the spring.[5] Hence from the variance of the motion and the expected thermal fluctuations we can determine the trapping stiffness (Equations S2 and S3)

$$\frac{1}{2}k\langle x^2\rangle = \frac{1}{2}k_B T \qquad\qquad \textbf{\textit{Eq. S2}}$$

$$k = \frac{k_B T}{\langle x^2\rangle} \qquad\qquad \textbf{\textit{Eq. S3}}$$

Hence from the variance of the particle motion along the different axis, the trapping stiffness can be determined.

Calculation of the radiation optical force

The time-averaged optical force (F) is a function of the spatial gradient of the electric field (E) and the induced polarization onto a BP-PDI dye molecule (P) is calculated as follows Equation S4:

$$< F(r,\omega) > = \frac{1}{2}Re\{\nabla E(r,\omega)\cdot P(r,\omega)\}, \qquad\qquad \textbf{\textit{Eq. S4}}$$

where r and ω are the spatial coordinates of the BP-PDI dye molecule and angular frequency of the laser, respectively. The electric field of a tightly focused laser beam with a high numerical aperture objective lens is expressed by an angular spectrum representation.[6] The induced polarization of the dye is derived from the density matrix equation beyond the perturbative regime with phenomenological damping constants.[18] The detailed energy diagram of dye molecules assumed in the calculation is obtained from the experimental spectroscopic measurements. The total optical force is calculated by multiplying the induced optical force on a single BP-PDI dye molecule with the number of dye molecules embedded inside a single PS MP.

Electronic Supplementary Information

Estimation of the temperature elevation of a single BP-PDI doped polystyrene microparticle trapped by a tightly focused 640 nm laser beam

Temperature distribution around a single optically-trapped PS MP was estimated in the following manner. The number of excitations per second for a single BP-PDI dye molecule is expressed by the Equation S5:

$$\text{Number of excitations per second } = \frac{C_{S_0} I_{ex}}{E_{ex}} \qquad \textbf{Eq. S5}$$

Where C_{S_0} is the absorption cross-section of the transition from S_0 to S_1 at 561 nm, I_{ex} is the irradiance of the 561-nm laser (in W m^{-2}), and E_{ex} is the energy of a photon at 561 nm. Hence, the duration when single BP-PDI is in the excited state in one second is given by the Equation S6:

$$\frac{C_{S_0} I_{ex} \tau_{S_1}}{E_{ex}} \qquad \textbf{Eq. S6}$$

Where τ_{S_1} is the fluorescence lifetime of BP-PDI. The absorbed energy at 640 nm by single BP-PDI molecule in the S_1 state per second, q_{SM}, is given by the Equation S7:

$$q_{SM} = \frac{C_{S_0} I_{ex} \tau_{S_1}}{E_{ex}} C_{S_1} I_{trap} \qquad \textbf{Eq. S7}$$

Where C_{S_1} is the absorption cross-section of the transition from S_1 to S_n at 640 nm and I_{trap} is the irradiance of the trapping laser at 640 nm. The absorbed energy at 640 nm by a single PS MP per second, Q, is then given by the Equation S8:

$$Q = N q_{SM} = N \frac{C_{S_0} I_{ex} \tau_{S_1}}{E_{ex}} C_{S_1} I_{trap} \qquad \textbf{Eq. S8}$$

Where, N is the number of BP-PDI molecules embedded inside the single PS MP. The absorbed energy will be mainly dissipated as heat to the surrounding environment from the single trapped particle. Thus, the present system can be regarded as the steady-state heat dissipation from a spherical heat source to the surrounding medium. The thermal diffusion equation of such system is expressed by equation S9.

$$\frac{dT(r)}{dr} = -\frac{Q}{4\pi\lambda}\frac{1}{r^2} \qquad \textbf{Eq. S9}$$

Where, r is the distance from the center of a polystyrene microparticle and λ is the thermal conductivity of water. As we are now considering CW photoirradiation with the trapping (640 nm) and excitation (561 nm) lasers, the system can be treated with the steady-state approximation. Under an assumption that the temperature inside a polystyrene microparticle is homogeneous, temperature distribution of this system $T(r)$ is given by the following Equations S10 (inside the microparticle) and S11 (outside the microparticle).

$$T(r) = T_0 = \frac{Q_{abs}}{4\pi\lambda} \frac{1}{r_{mp}} + T_{room} \quad (0 \le r \le r_{MP}) \quad \boldsymbol{Eq.S10}$$

$$= \frac{Q_{abs}}{4\pi\lambda} \frac{1}{r} + T_{room} \quad (r_{MP} < r) \quad \boldsymbol{Eq.S11}$$

Where, T_{room} is a room temperature, r_{mp} is the radius of the trapped PS MP.

Figure S9 shows the spatial distribution of temperature, $T(r)$. Note that the molar absorption coefficients of BP-PDI in the excited state (S$_1$) at 640 nm cannot be directly determined from transient absorption spectrum because of the stimulated emission signal is remarkable compared with transient absorption signal (see Figure 1B in the main text). Therefore, ϵ_{S_1} at 700 nm is approximately used in this estimation. The $T(r)$ is calculated using the following values: molar absorption coefficients of BP-PDI in the ground state (S$_0$) at 561 nm, $\epsilon_{S_0} = 5 \times 10^4$ M^{-1}·cm^{-1}, and in the excited state (S$_1$) at 700 nm, $\epsilon_{S_1} = 1 \times 10^4$ M^{-1}·cm^{-1}, $I_{ex} = 1 \times 10^7$ W·m^{-2}, $I_{trap} = 1.3 \times 10^{10}$ W·m^{-2} (corresponding to 10 mW incident power focused into a spot of 1 μm of diameter), $\tau_{S_1} = 6 \times 10^{-9}$ s, $N = 1.3 \times 10^6$ dyes/MP, $\lambda = 0.60$ W·m^{-1}·K^{-1}, $r_{MP} = 0.5 \times 10^{-6}$ m, and $T_{room} = 294.15$ K.

In one hand, the temperature elevation for the most unfavorable condition is of roughly of 5 K on the surface of the PS MP. On the other hand, the temperature elevation for the most favorable condition is of only 0.5 K. Moreover, as above-mentioned, the temperature elevation is calculated considering the absorption cross-section (C_{S1}) at 700 nm as the C_{S1} at 640 nm cannot be directly determined from the transient absorption spectrum due to the stimulated emission signal. However, considering that the contribution of SE is much larger at 640 nm than at 700 nm, the temperature elevation should be much smaller than the temperature estimated above. Therefore, we do not expect a strong heating effect on the observed phenomena.

Electronic Supplementary Information

Detailed description of red- and blue- detuned laser on optical resonance effect

The sign of the gradient force is determined by the phase relation between the laser and the induced polarization. Typically, for ground state excitation, the red-detuned laser (longer wavelength than the absorption peak) is in phase with the induced polarization. Therefore, concerning the electromagnetic interaction, it is potentially favorable, and the attractive gradient force is generated toward the focal center.

Instead, if the laser is blue-detuned (laser wavelength slightly shorter than the absorption peak), the phase of laser and the induced polarization are out of phase. Therefore, the electromagnetic interaction becomes potentially unfavorable at the focal center, and a repulsive gradient force will be generated. Instead, for the stimulated emission (SE) process, which start from a higher to a lower energy level, the phase of the induced polarization flips. Namely, the red-detuned laser generates a repulsive gradient force because the phase relation is out of phase, and the blue-detuned laser generates the attractive gradient force since both laser and induced polarization are in phase.

Electronic Supplementary Information

Supplementary Tables:

Table S1: BP-PDI molecule loading per microparticle in function of the dyeing cycles.

	1st Cycle	2nd Cycle	3rd Cycle	4th Cycle	5th Cycle
BP-PDI loading (molecules/MPs)	4.4 x 10^5	8.6 x 10^5	9.8 x 10^5	11.6 x 10^5	12.8 x 10^5

Table S2: Relation between the dipole moment and the oscillator strength for all the fitted transitions. Equation S12 is used for estimating the experimental transition dipole moment (μ) from the experimental oscillator strength (f), where h, e, m_e, and ν are the Plank constant, the electronic charge, the electron mass, and the frequency of the transition energy, respectively.

Electronic Transition	Experimental Oscillator Strength	Experimental Transition Dipole Moment / D
1-4	0.27	5.70
2-4	0.23	5.44
3-4	0.082	3.38

$$\mu = \left(\frac{3he^2}{8\pi^2 m_e \nu} f \right)^{\frac{1}{2}}, \qquad Eq.\,S12$$

Electronic Supplementary Information

Supplementary Figures:
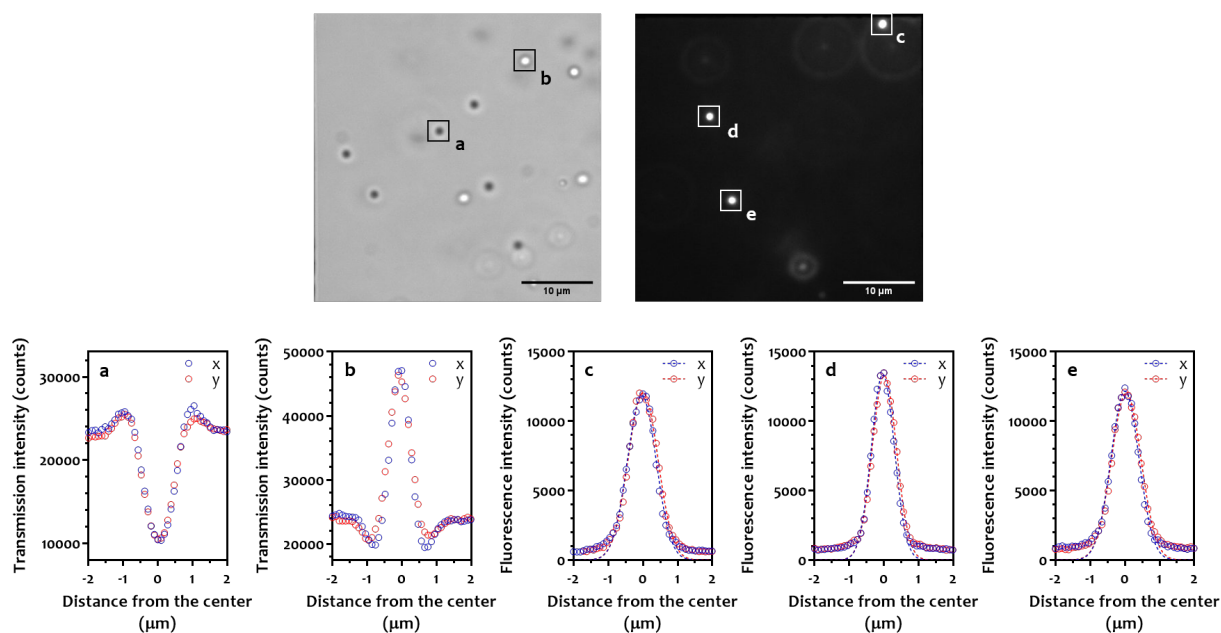
Figure S1 Top: Representative transmission and fluorescence image of the BP-PDI dye doped polystyrene microparticle suspended in water. λ_{WF} = 561 nm. The scale bar is 10 μm. Bottom: (a-b): Changes in the transmission intensity along x- and y- directions for MPs a (the MP is located below the imaging plane) and b (the MP is located above the imaging plane). (c-e): Changes in the fluorescence intensity along the x- and y- direction for MPs c, d, and e. The fluorescence intensity profile can be fitted with a single Gaussian function ($R^2 > 0.99$), which indicates that the BP-PDI dye molecules are homogeneously distributed inside the MP. The height of the curve peak is 11900 ± 1500 counts, which indicates that the BP-PDI dye loading is similar for all the MPs (deviation values smaller than 13%). The fitted full width at half maximum (FWHM) is 0.92 ± 0.06 μm (n=30) for both x-, and y- directions, when the MPs are focused at the imaging plane. The fitted FWHM indicates that the size of the MPs after the swallowing process is approximately 1 μm, maintaining their initial size. The fitted flattening for the MPs is 0.01 ± 0.05 (n=30), also when the MPs are focused at the imaging plane. This near-zero flattening value indicates that the shape of the MPs has not significantly changed during all the swallowing process, keeping their spherical shape.

Magnification x10000

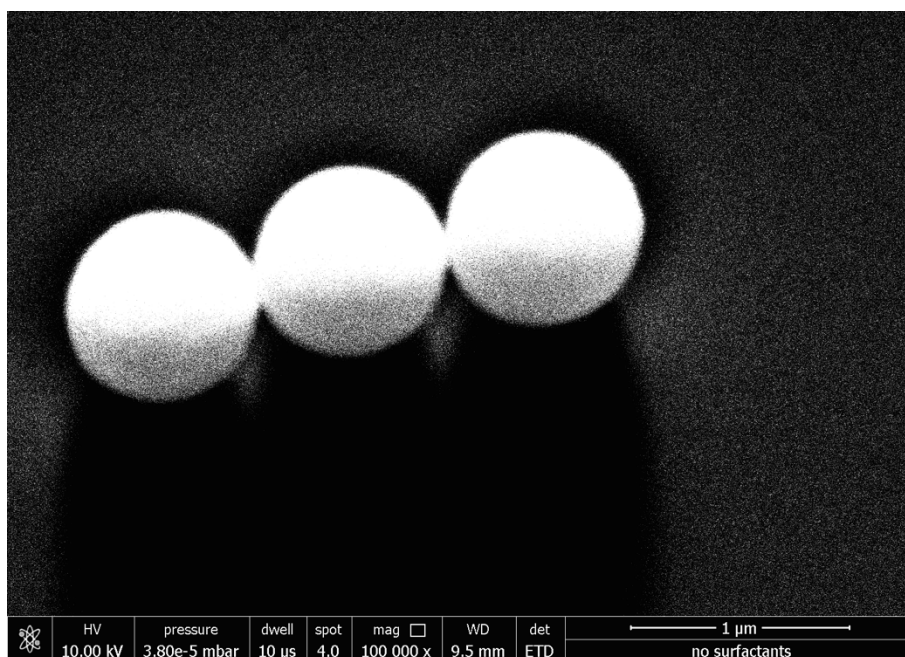| HV	pressure	dwell	spot	mag ☐	WD	det	10 µm
10.00 kV	4.07e-5 mbar	3 µs	4.0	10 000 x	9.4 mm	ETD	no surfactants

Magnification x100000

HV	pressure	dwell	spot	mag ☐	WD	det	1 µm
10.00 kV	3.80e-5 mbar	10 µs	4.0	100 000 x	9.5 mm	ETD	no surfactants
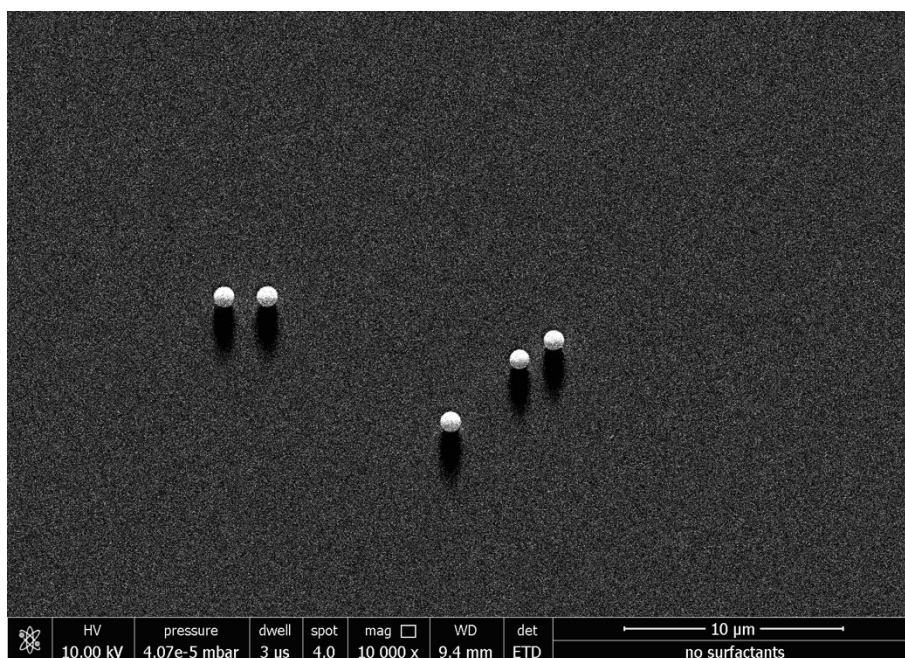
Figure S2: Scanning electron image for the BP-PDI doped polystyrene particles. Top: The used magnification is x10000. The average size of the particles is 890 ± 20 nm (n = 30 particles). Bottom: The used magnification is x100000. As can be observed from the images, the particles are completely spherical, and their polydispersity index is small.

x-z Projection

x-y Projection

0.5 µm

y-z Projection
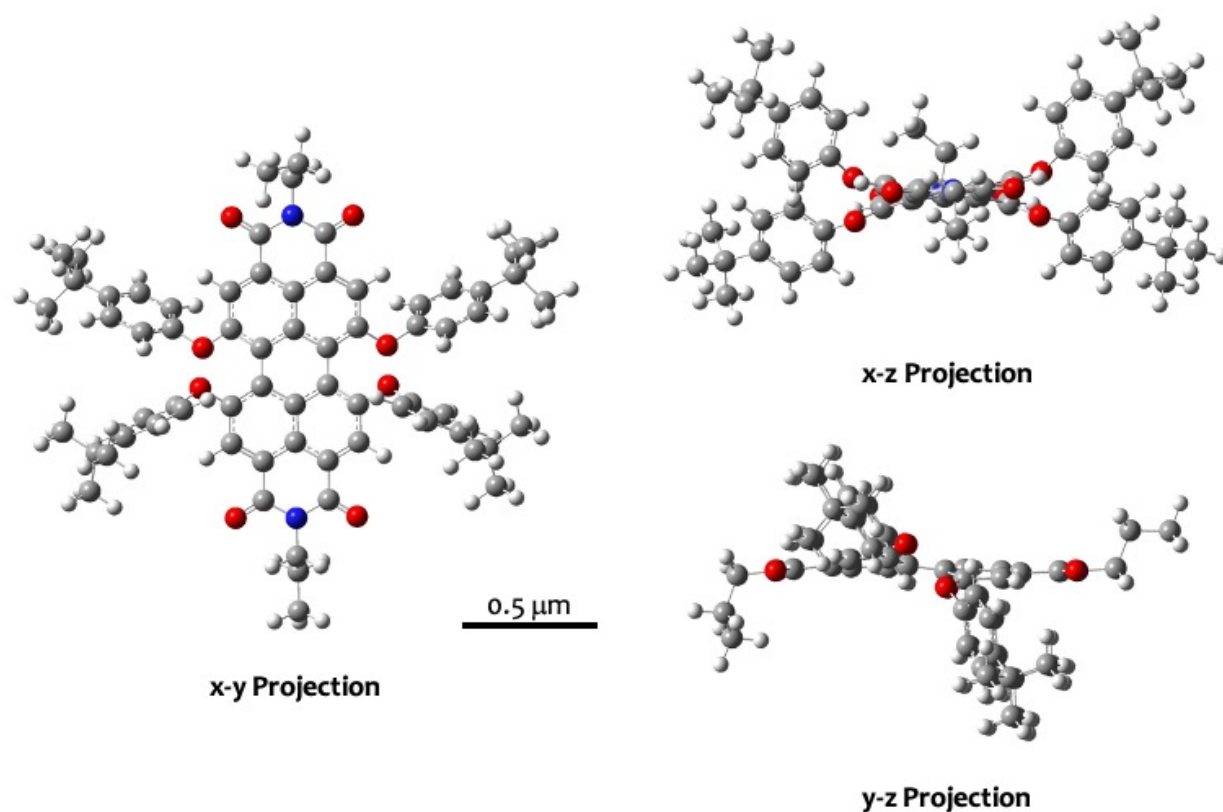
Figure S3 3D optimized chemical structure of BP-PDI at the AM1 level of theory.[1] The molecule geometry has been optimized using Gaussian 03 suite.[8] The optimized geometry has been proved as a local minimum structure, because there are no modes with imaginary frequency. Afterwards, the BP-PDI volume has also been calculated using Gaussian 03 suite, estimating a value of 803 cm^3/mol = 1.33 nm^3/molecule.
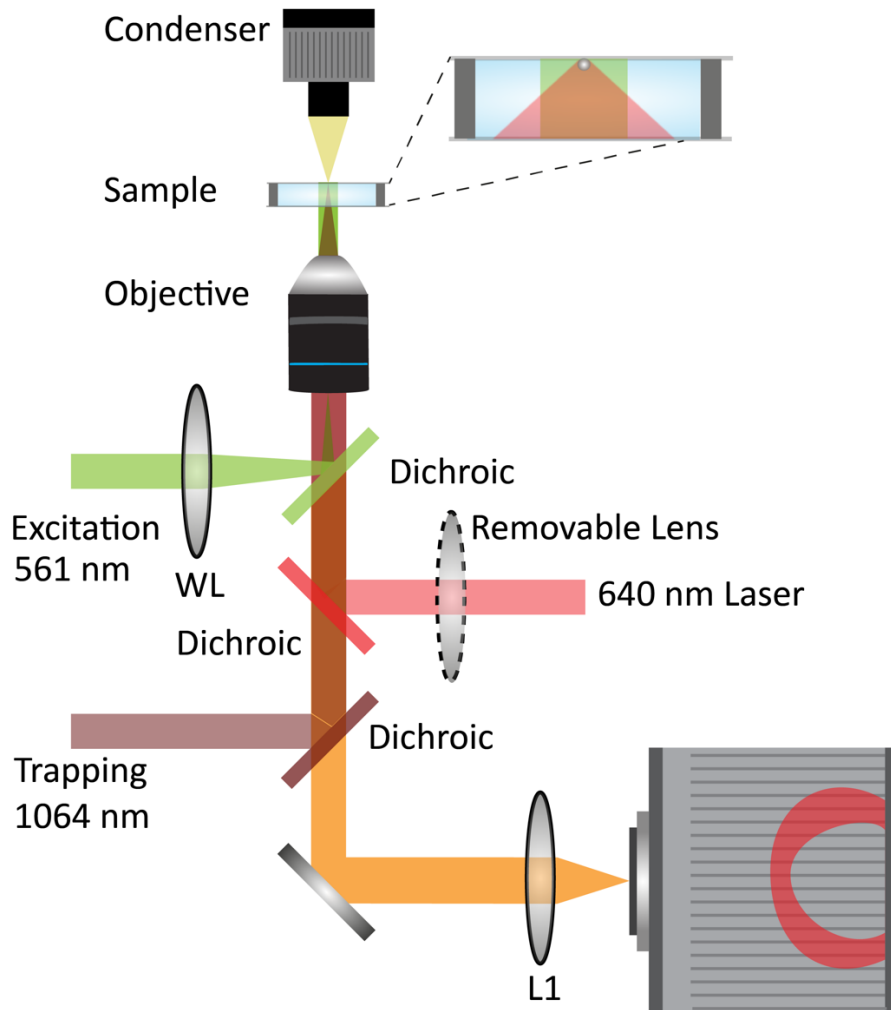
Figure S4: Optical trap, Stimulated emission, Wide-field microscope. A 561 nm laser is focused at the back aperture of the objective to excite the sample with widefield configuration. A 640 nm laser is available for widefield illumination and trapping which is enabled by a removable lens. A 1064 nm laser is also available for trapping. Upper right: Sketch of the optical condition used in this work. The sample chamber is sandwiched by two glass coverslips. The trapping laser is focused at the upper glass/solution interface and the widefield laser(s) irradiates homogeneously the surroundings of the trapping spot. A sequence of three dichroic mirrors (DMSP605 from Thorlabs, 89402x from Chroma Technology Corp, and DMLP950 from Thorlabs) and a careful selection of the optical path have been engineered to ensure the correct use the three lasers simultaneously. The fluorescence emitted by the fluorescent PS MPs is collected by the objective lens and filtered using the suitable optical filters to remove the back-reflection of the different used laser(s). Finally, the image is projected by the tube lens (L1) on a sCMOS camera.
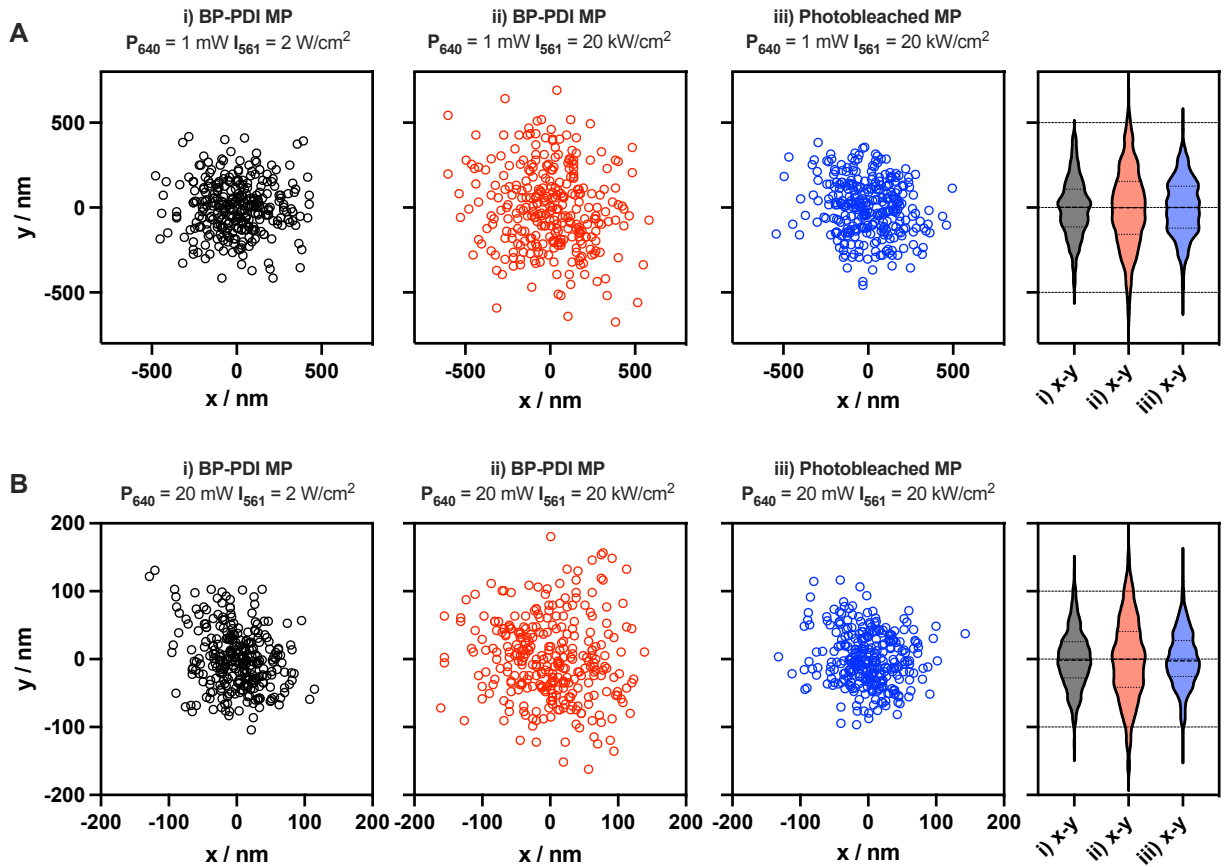
Figure S5 Left: representative examples of a single trapped MP motion at the glass/solution interface for selected experimental conditions over 4 seconds (100 fps). A) P_{640} = 1 mW. B) P_{640} = 20 mW. i) I_{561} = 2 W/cm^2, BP-PDI MP; ii) I_{561} = 20 kW/cm^2, BP-PDI MP; iii) I_{561} = 20 kW/cm^2, photobleached MP. Right: Violin plot for the x,y- MP position distributions measured at the selected experimental conditions.
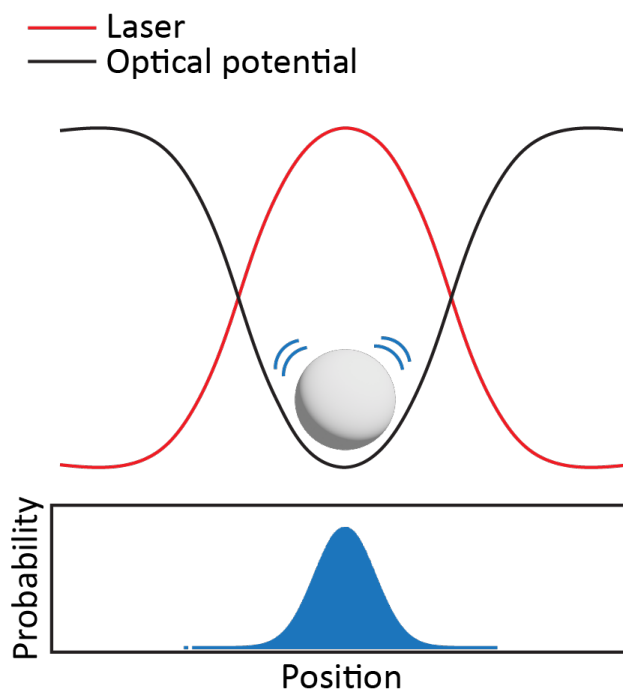
Figure S6 Optical trapping stiffness determination. Cartoon representation of the optical laser field approximated as a gaussian (red curve) and the resulting optical potential (black curve). The trapping stiffness can be determined from the variance of the particle movement inside the optical potential.
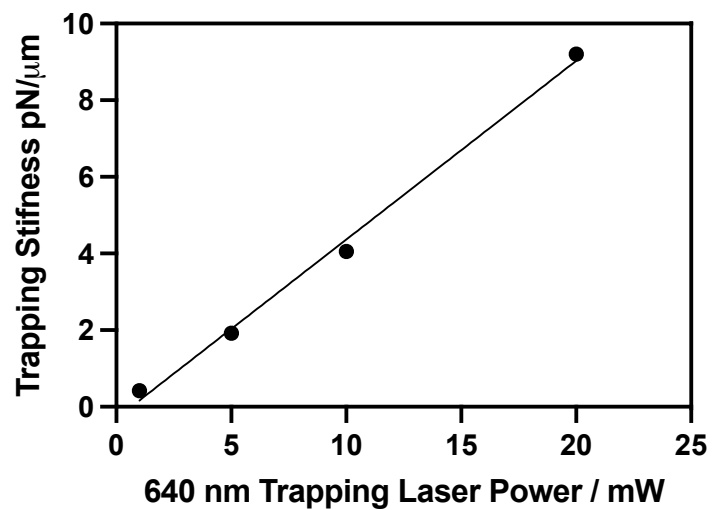
Figure S7 Trapping stiffness as the function of the 640 nm trapping laser power for a single trapped BP-PDI doped PS MP in absence of the 561 nm widefield excitation.
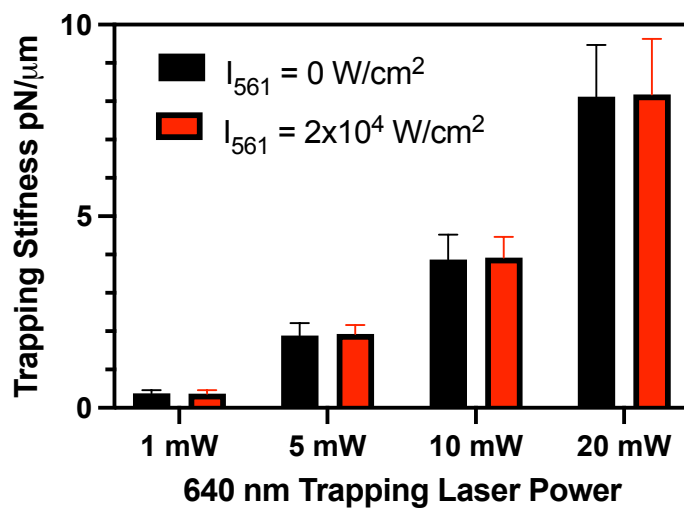
Figure S8 Trapping stiffness of a single trapped bare PS MP as the function of the 640 nm trapping laser power and the 561 nm widefield irradiance (black bar = 0 W/cm^2; red bar = 2 x 10^4 W/cm^2).
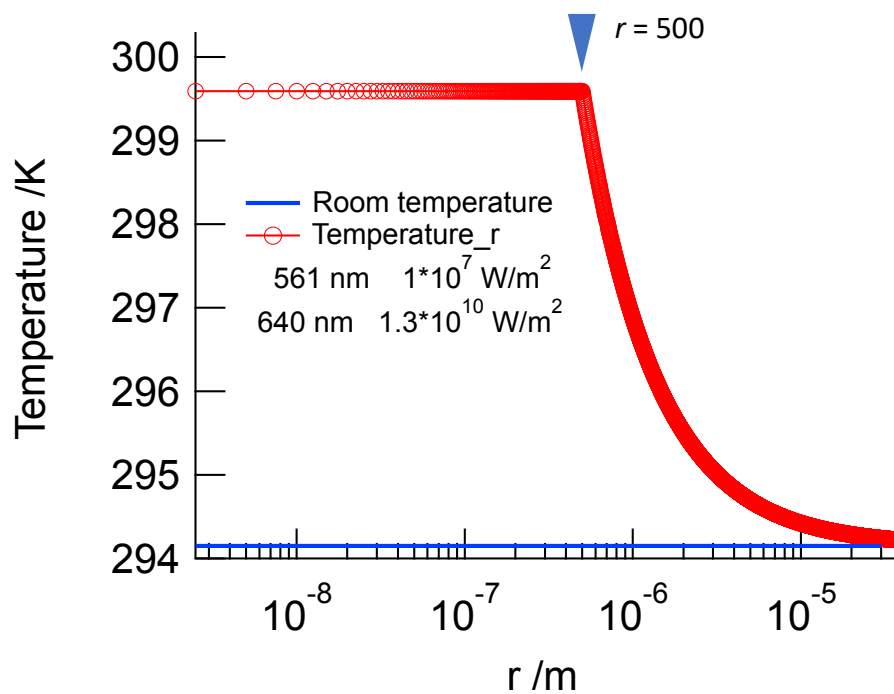
Figure S9 Temperature distribution inside and around a single optically trapped BP-PDI PS MP containing CW photoexcitation at 561 nm. The MP is trapped in water by a focused CW 640 nm laser. Detailed calculation procedure and parameters are described in a previous section of the Supplementary Information.
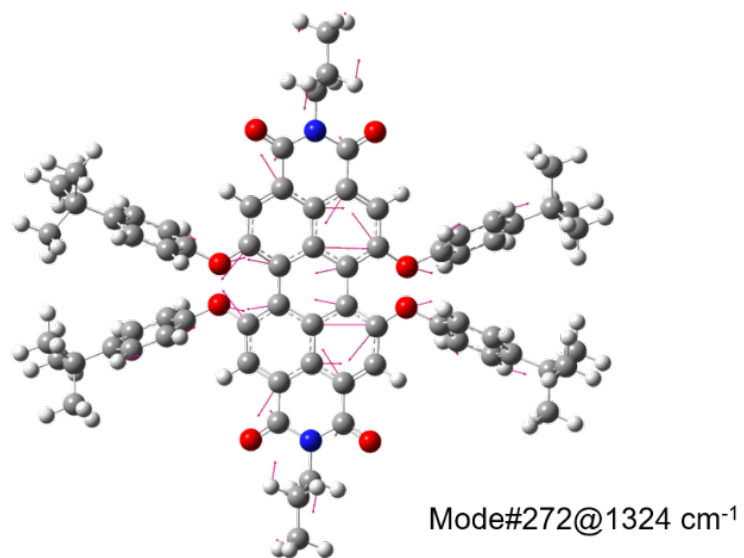
Mode#272@1324 cm^{-1}

Figure S10 Nuclear displacement of a C-C stretching mode at 1324 cm^{-1} calculated at the B3LYP level of theory using the 6-31G(d) basis set.
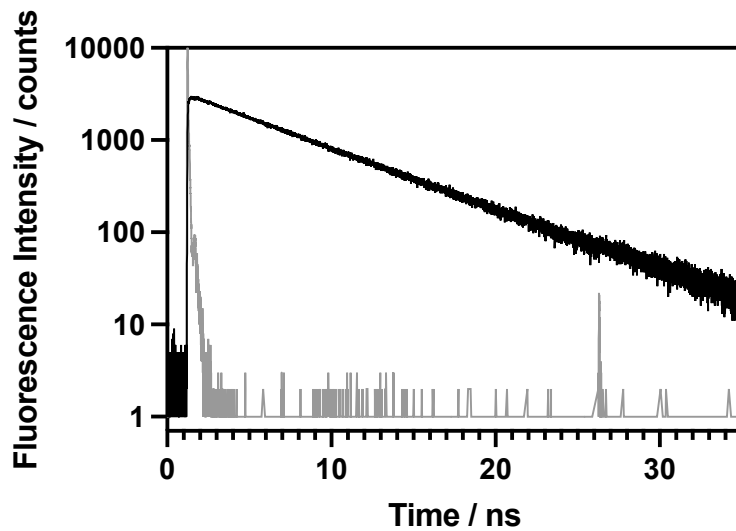
Figure S11 Time-resolved fluorescence decay trace for BP-PDI dye. The grey trace represents the instrument response function (IRF). BP-PDI molecules were excited at 532 nm and its fluorescence recorded at 603 nm.
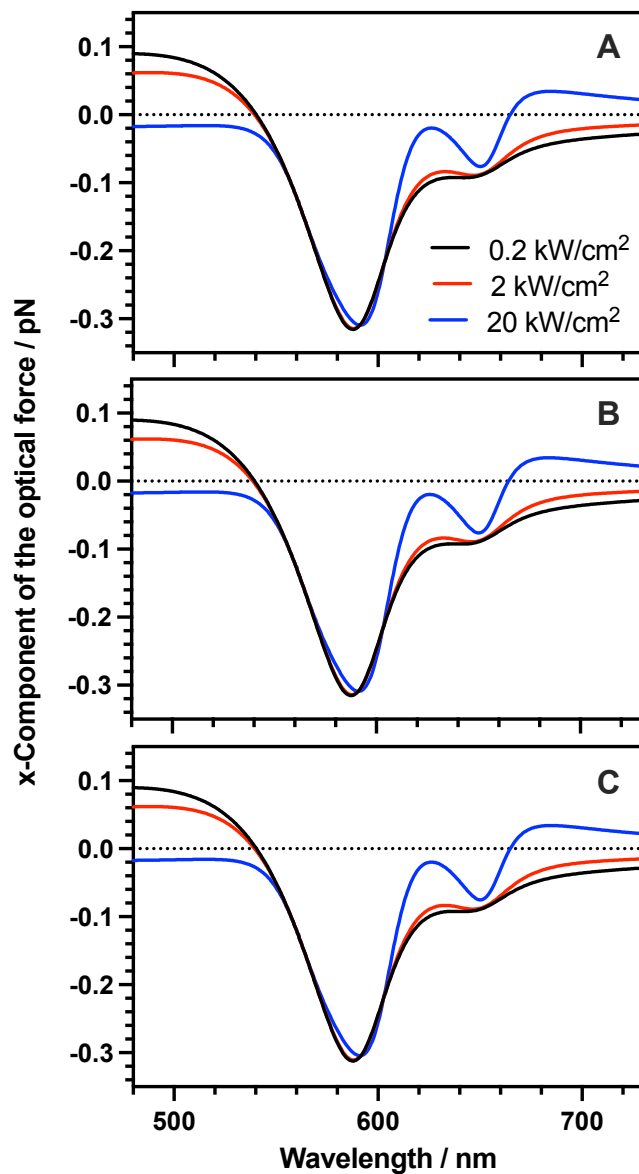
Figure S12 Optical force spectra for different vibrational relaxation lifetimes (0.15, 1.5 and 15 ps for A, B and C, respectively) and 561 nm excitation irradiance (black, red, and blue lines for 0.2, 2, and 20 kW/cm^2, respectively). For all the calculations, the BP-PDI molecule is fixed at (x, z) = (+120, 0) nm and we considered that the center of the tightly focused laser beam is the origin of the coordinate system.
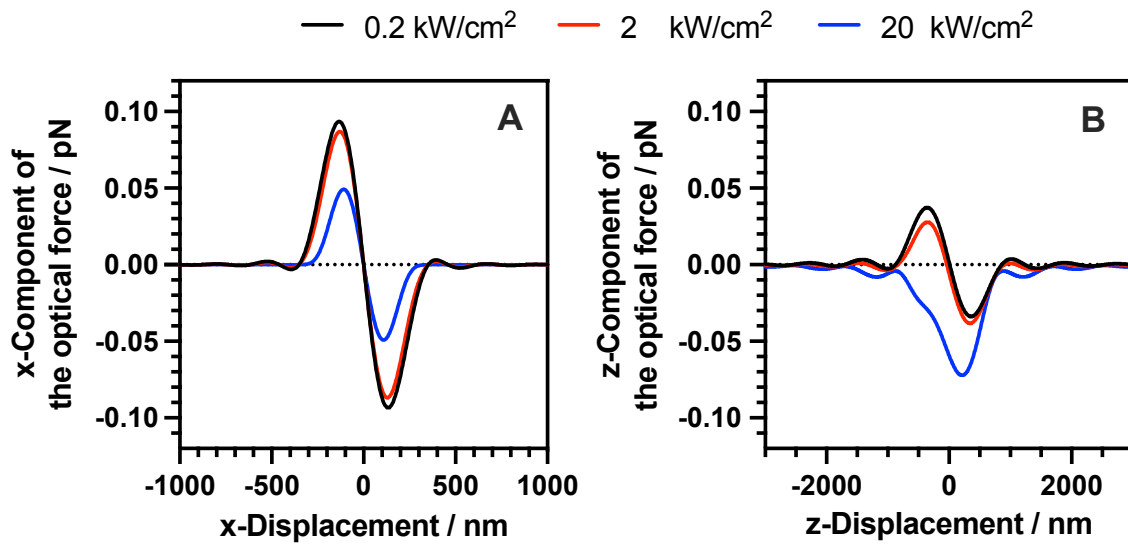
Figure S13: Spatial dependence of the gradient force along the (A) x- and (B) z-axis when the 561 nm wide-field irradiance is 0.2 kW/cm², 2 kW/cm², and 20 kW/cm² (black, red, and blue lines, respectively). The 640 nm trapping laser power is set at 2 mW. The ORE gradient force becomes maximum approximately at the position of ± 120 nm (x-direction) and ± 300 nm (z-direction) away from the center of the laser focus. Of note, the direction and sign of the induced optical is calculated along the x-,z-direction. Thus, plus and minus optical forces are directed to the focus from minus x/z and plus x/z positions, respectively. In the Main Text, we calculated the optical force spectrum at this point to maximize the induced ORE force.
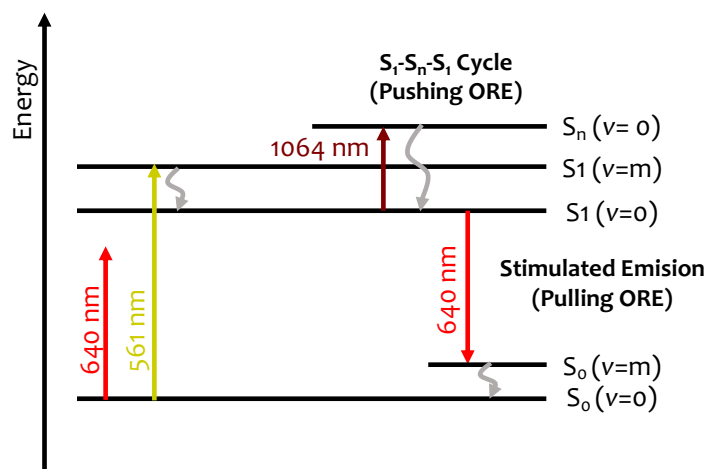
Figure S14: Jablonski diagram of BP-PDI electronic states involved in the three-laser system: i) a 561 nm widefield laser will excite the BP-PDI molecules from S_0 to S_1; ii) a 640 nm widefield laser will promote the stimulated emission from S_1 (pulling repulsive ORE); and iii) a 1064 nm trapping laser to trap the BP-PDI doped PS MPs and simultaneously induce the S_1–S_n–S_1 resonance cycle (pushing attractive ORE).

Electronic Supplementary Information

<u>Supplementary bibliography</u>

[1] T. Behnke, C. Würth, K. Hoffmann, M. Hübner, U. Panne, U. Resch-Genger, U. Encapsulation of hydrophobic dyes in polystyrene micro- and nanoparticles via swelling procedures. *J. Fluoresc.* **2011**, *21*, 937–944.

[2] Koga, M.; Sotome, H.; Ide, N.; Ito, S.; Nagasawa, Y.; Miyasaka, H. Direct determination of molar absorption coefficients of several molecules in the lowest excited singlet states, *Photochem. Photobiol. Sci.* **2021**, *20*, 1287-1297.

[3] Louis, B.; et al. Fast-tracking of single emitters in large volumes with nanometer precision. *Opt. Express* **2020**, *28*, 28656–28671.

[4] Louis, B.; et al. Unravelling 3D dynamics and hydrodynamics during incorporation of dielectric particles to an optical trapping site. *ACS Nano* **2023**, 17, 3797–3808.

[5] Berg-Sorensen, K.; Oddershede, L.; Florin, E. L.; Flyvbjerg, H. Unintended filtering in a typical photodiode detection system for optical tweezers. *J. Appl. Phys.* **2003**, *93*, 3167−3176.

[6] Novotny, L.; Hecht, B. Propagation and focusing of optical fields. Principles of Nano-Optics; Cambridge University Press, **2006**; pp 45−88.

[7] M.J.S. Dewar, E.G. Zoebisch, E.F. Healy, and J.J.P. Stewart, Development and use of quantum mechanical molecular models. 76. AM1: a new general purpose quantum mechanical molecular model. *J. Am. Chem. Soc.* **1985**, 107, 13, 3902–3909.

[8] M.J. Frisch, G.W. Trucks, H.B. Schlegel, G.E. Scuseria, M.A. Robb, J.R. Cheeseman, J.A. Montgomery, Jr., T. Vreven, K.N. Kudin, J.C. Burant, J.M. Millam, S.S. Iyengar, J. Tomasi, V. Barone, B. Mennucci, M. Cossi, G. Scalmani, N. Rega, G.A. Petersson, H. Nakatsuji, M. Hada, M. Ehara, K. Toyota, R. Fukuda, J. Hasegawa, M. Ishida, T. Nakajima, Y. Honda, O. Kitao, H. Nakai, M. Klene, X. Li, J.E. Knox, H.P. Hratchian, J.B. Cross, V. Bakken, C. Adamo, J. Jaramillo, R. Gomperts, R.E. Stratmann, O. Yazyev, A.J. Austin, R. Cammi, C. Pomelli, J.W. Ochterski, P.Y. Ayala, K. Morokuma, G.A. Voth, P. Salvador, J.J. Dannenberg, V.G. Zakrzewski, S. Dapprich, A.D. Daniels, M.C. Strain, O. Farkas, D.K. Malick, A.D. Rabuck, K. Raghavachari, J.B. Foresman, J.V. Ortiz, Q. Cui, A.G. Baboul, S. Clifford, J. Cioslowski, B.B. Stefanov, G. Liu, A. Liashenko, P. Piskorz, I. Komaromi, R.L. Martin, D.J. Fox, T. Keith, M.A. Al-Laham, C.Y. Peng, A. Nanayakkara, M. Challacombe, P.M.W. Gill, B. Johnson, W. Chen, M.W. Wong, C. Gonzalez, and J.A. Pople, Gaussian 03, Revision C.02, Gaussian, Inc., Wallingford CT, **2004**.